

Supporting Information

Relation between blood pressure and pulse wave velocity for human arteries

Yinji Ma[†], Jungil Choi[†], Aurélie Hourlier-Fargette, Yeguang Xue, Ha Uk Chung, Jong Yoon Lee, Xiufeng Wang, Zhaoqian Xie, Daeshik Kang, Seungyong Han, Heling Wang, Seung-Kyun Kang, Yisak Kang, Xinge Yu, Marvin J. Slepian, Milan S. Raj, Jeffrey B. Model, Xue Feng, Roozbeh Ghaffari, John A. Rogers, and Yonggang Huang**

Note 1. The relation between P and A

Figures 1B and C show the schematic diagram of the artery cross section before (initial thickness h_0 and radius R_0 in Fig. 1B) and after (thickness h and radius R in Fig. 1C) the deformation due to the blood pressure (P). In the cylindrical coordinates $\{r, \theta, z\}$, the true stress and logarithmic strain are $\{\sigma_{rr}, \sigma_{\theta\theta}, \sigma_{zz}\}$ and $\{\varepsilon_{rr}, \varepsilon_{\theta\theta}, \varepsilon_{zz}\}$ at any point Q (r_0 and r before and after the deformation, respectively). The linear elastic constitutive model gives $\sigma_{\theta\theta} - \sigma_{rr} = [E/(1+\nu)](\varepsilon_{\theta\theta} - \varepsilon_{rr})$. In the *in vitro* experiments the tube length ($\sim 2\text{m}$) is much larger than its radius ($\sim 6\text{ mm}$) such that the plane-strain model is adopted (i.e., the axial strain $\varepsilon_{zz} = 0$), which together with the material incompressibility, give $\varepsilon_{rr} = -\varepsilon_{\theta\theta}$ such that

$$\sigma_{\theta\theta} - \sigma_{rr} = \bar{E}\varepsilon_{\theta\theta}, \quad (\text{S1})$$

where the plane-strain modulus $\bar{E} = E/(1-\nu^2)$ is related to the linear elastic modulus E and Poissons' ratio $\nu = 0.5$ of the tube, and the logarithmic strain $\varepsilon_{\theta\theta} = \ln(r/r_0)$. Substitution of Eq. S1 into Eq. 4 yields

$$\begin{aligned}
P &= \int_{R^2}^{(R+h)^2} \frac{1}{2} (\sigma_{\theta\theta} - \sigma_{rr}) \frac{dr^2}{r^2} \\
&= \int_{R^2/R_0^2}^{(R+h)^2/(R_0+h_0)^2} \left[-\frac{\ln \lambda^{1/2}}{2\lambda(\lambda-1)} \right] d\lambda,
\end{aligned} \tag{S2}$$

which leads to Eq. 6, where the inner radii R_0 and R of the artery area before and after the deformation are related to the corresponding inner areas by $A_0 = \pi R_0^2$ and $A = \pi R^2$.

For the human artery characterized by the Fung hyperelastic model with the axial strain E_{zz} and strain in the circumferential direction $E_{\theta\theta} = (e^{2\varepsilon_{\theta\theta}} - 1)/2$, the constitutive model gives

$$\sigma_{\theta\theta} - \sigma_{rr} = \frac{\partial W}{\partial \varepsilon_{\theta\theta}} = \frac{1}{2} C e^{a_2 E_{zz}^2} a_1 (e^{2\varepsilon_{\theta\theta}} - 1) e^{2\varepsilon_{\theta\theta} + \frac{1}{4} a_1 (e^{2\varepsilon_{\theta\theta}} - 1)^2}, \tag{S3}$$

where W given in Eq. 9 is for two-dimensional analysis, and the left hand side of the above equation results from the stress state $\{\sigma_{rr}, \sigma_{\theta\theta}, \sigma_{zz}\}$ subtracted by a hydrostatic stress $\{\sigma_{rr}, \sigma_{rr}, \sigma_{rr}\}$, i.e., $\{0, \sigma_{\theta\theta} - \sigma_{rr}, \sigma_{zz} - \sigma_{rr}\}$ for this incompressible material. Substitution of Eq. S3 into Eq. 4 yields

$$\begin{aligned}
P &= \int_{R^2}^{(R+h)^2} \frac{1}{2} (\sigma_{\theta\theta} - \sigma_{rr}) \frac{dr^2}{r^2} \\
&= \int_{R^2/R_0^2}^{(R+h)^2/(R_0+h_0)^2} \left[-\frac{1}{4} C e^{a_2 E_{zz}^2} a_1 e^{\frac{1}{4} a_1 (\lambda-1)^2} \right] d\lambda,
\end{aligned} \tag{S4}$$

which can be simplified to Eq. 10.

Note 2. The effect of liquid viscosity in the tube

For the tube [$h_0 = 0.29$ mm, $R_0 = 6.35$ mm, and 15:1 PDMS (580kPa)], both water (viscosity $\mu = \sim 0.001$ Pa·s and density $\rho = 1000$ kg/m³) and water/glycerol mixture (viscosity $\mu = \sim 0.006$ Pa·s and density $\rho = 1130$ kg/m³) are used as the liquid in the tube in the experiments. Figure S3 shows that the PWV for water/glycerol mixture is slightly smaller than that for water at

the same pressure. The present model, which accounts for the effect of mass density but not viscosity of the liquid, agrees well with the experiments without any parameter fitting. This suggests that the effect of the liquid viscosity may be small, considering the viscosities of two liquids are different by a factor of 6. The viscosity of the blood is ~ 0.004 Pa·s, between those of water and water/glycerol mixture, such that its effect on human's PWV should also be small.

Note 3. The asymptote of P and PWV at large A

For a large ratio A/A_0 , the first term $e^{a_1(A-A_0)^2/(4A_0^2)}/A_0$ inside the square root on the right hand side of Eq. 11 overwhelms the second term $e^{a_1(A-A_0)^2/[4(A_0+A_{wall})^2]}/(A_0+A_{wall})$. Therefore, at $E_{zz}=0$, Eq. 11 has the asymptote

$$PWV^2 \sim \frac{Ca_1}{4\rho} \frac{A}{A_0} e^{\frac{a_1(A-A_0)^2}{4A_0^2}}. \quad (S5)$$

The function $\operatorname{erfi}(x)$ has the asymptote $e^{x^2}/(\sqrt{\pi}x)$ [20] at a large x . Similarly, at $E_{zz}=0$, Eq. 10 has the asymptote

$$P \sim \frac{C}{2} \frac{A_0}{A-A_0} e^{\frac{a_1(A-A_0)^2}{4A_0^2}}, \quad (S6)$$

because the second term $\operatorname{erfi}\left\{\sqrt{a_1}(A-A_0)/[2(A_0+A_{wall})]\right\}$ of the right hand side of Eq. 10 is overwhelmed by the first term $\operatorname{erfi}\left[\sqrt{a_1}(A-A_0)/(2A_0)\right]$ for a large A/A_0 . The ratio of Eq. S5 to Eq. S6 gives

$$\frac{PWV^2}{P} = \frac{a_1}{2\rho} \left[\frac{A(A-A_0)}{A_0^2} \right], \quad (S7)$$

which is a quadratic equation for A/A_0 , and has the solution

$$\frac{A}{A_0} = \frac{1}{2} + \sqrt{\frac{1}{4} + \frac{2\rho}{a_1} \frac{PWV^2}{P}}. \quad (\text{S8})$$

Its substitution into Eq. S6 yields Eq. 17.

SI figure captions

Figure S1. Storage E' and loss moduli E'' of the 17:1 PDMS versus the frequency in the range 0.1 HZ~10 HZ.

Figure S2. True stress versus logarithmic strain of the 17:1 PDMS, which is linear elastic for the strain up to 30%.

Figure S3. The pressure versus PWV in the *in vitro* experiments [$h_0 = 0.29$ mm, $R_0 = 6.3$ mm, and 15:1 PDMS (580kPa)] for different liquids. The results for the present model are also shown.

Figure S4. BioStamp® on (A) torso in the sub-clavicular region and (B) posterior side overlaying the scapula.

Figure S5. $1/\Delta t$ and DBP versus time during the post-exercise period.

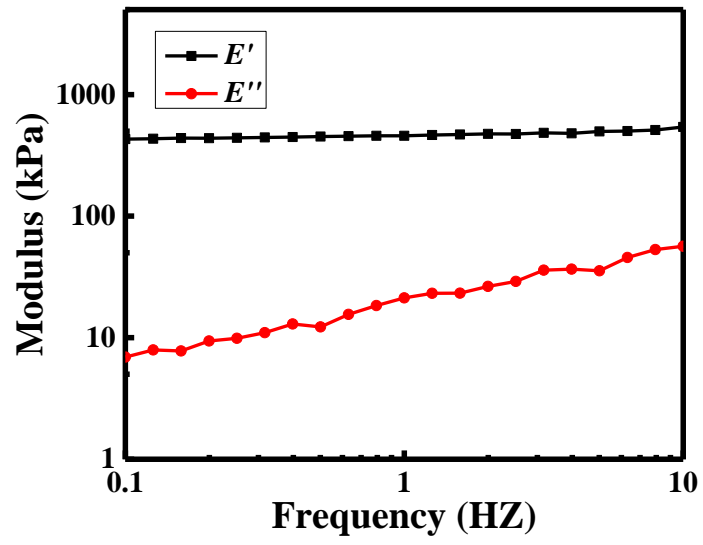


Figure S1

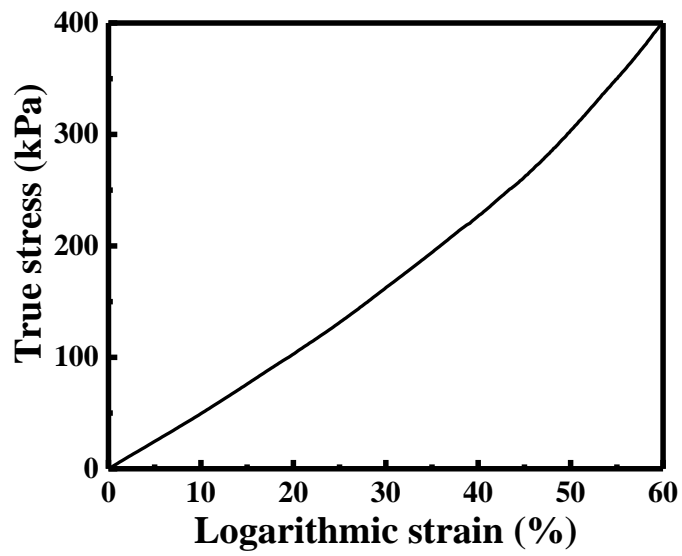


Figure S2

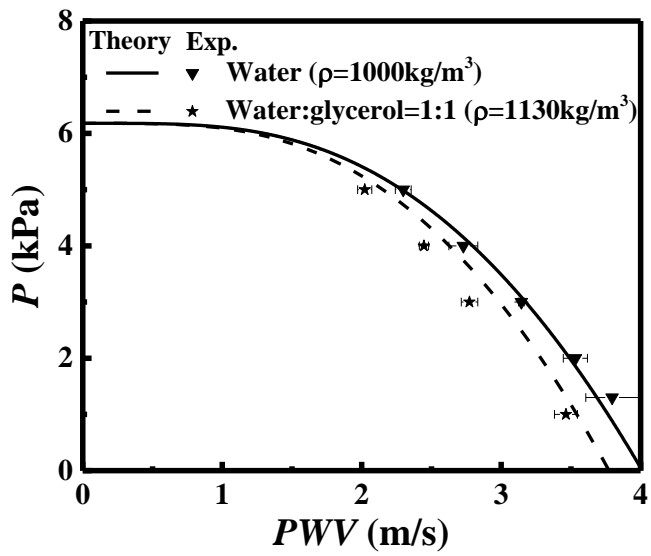


Figure S3



Figure S4

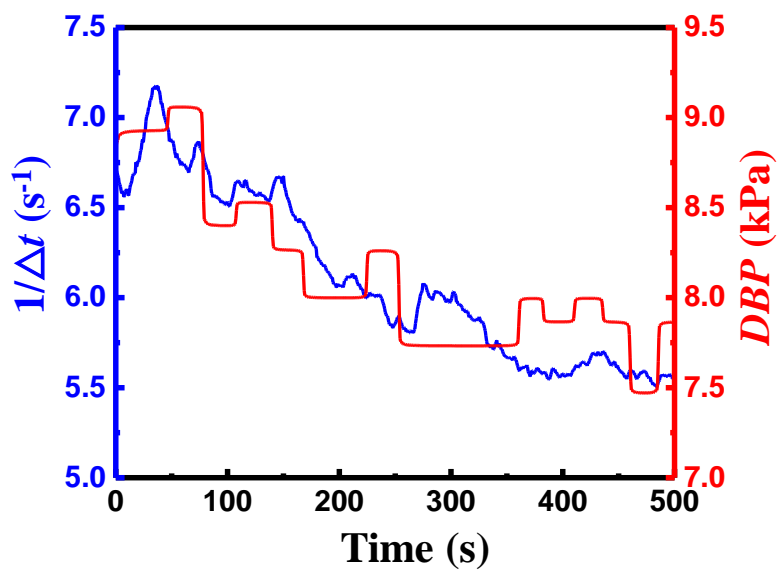


Figure S5